doi: 10.1111/j.1751-3928.2008.00076.x *Resource Geology* Vol. 59, No. 1: 1–14

Original Article

Geology and Origin of Supergene Ore at the Lavrion Pb-Ag-Zn Deposit, Attica, Greece

Nikos Skarpelis and Ariadne Argyraki

Department of Economic Geology and Geochemistry, Faculty of Geology and Geoenvironment, University of Athens, Panepistimiopoli, Zografou, Greece

Abstract

The Lavrion carbonate-hosted Pb-Ag-Zn deposit in southeast Attica, Greece, consisted of significant non-sulfide ore bodies. The polymetallic sulfide mineralization was subjected to supergene oxidation, giving rise to gossan. The principal non-sulfide minerals of past economic importance were smithsonite, goethite and hematite. The supergene mineral assemblages occupy secondary open spaces and occur as replacement pods within marble. Calamine and iron ore mainly filled open fractures. X-ray diffraction and scanning electron microscopy of samples of oxidized ore indicate complex gossan mineralogy depending on the hypogene mineralogy, the degree of oxidation and leaching of elements, and the local hydrologic conditions. Bulk chemical analysis of the samples indicated high ore-grade variability of the supergene mineralization. On multivariate cluster analysis of geochemical data the elements were classified into groups providing evidence for their differential mobilization during dissolution, transport and re-precipitation. The mode of occurrence, textures, mineralogy and geochemistry of the non-sulfide mineralization confirm that it is undoubtedly of supergene origin: the product of influx into open fractures in the country rock of highly acidic, metal-rich water resulting from the oxidation of pyrite-rich sulfide protore. Dissolution of carbonates led to opening of the fractures. Mineral deposition in the supergene ore took place under near-neutral to mildly acidic conditions. The supergene dissolution and re-precipitation of Fe and Zn in the host marble increased metal grades and separated iron and zinc from lead, thereby producing economically attractive deposits; it further contributed to minimization of pollution impact on both soil and ground water.

Keywords: calamine, gossan, Greece, Lavrion, non-sulfide ore, smithsonite, supergene ore.

1. Introduction

Ancient miners at Lavrion were interested in exploitation of Ag-rich ore. Silver and lead production in ancient times (until the first century BC) amounted to 3500 t and 1,400,000 t, respectively. According to calculation, the tonnage of ancient slag found in the area in 1864 was 1,500,000 t containing 10% Pb and 50 g/t Ag. The tonnage of ore waste was estimated at 10,000,000 t containing 7% Pb and 140 g/t Ag (Conofagos, 1980). Additional Zn-rich mineral waste (sphalerite and smithsonite) remained either at surface or underground. The large amounts of Pb- and Ag-rich slag and the mineral waste were processed and smelted after the reactivation of the mines in 1864.

Minor exploitation and processing of iron ore in ancient times took place during the classical era. The clamps and dowels of the Erectheion (Acropolis, Athens) as well as various tools necessary for exploration and exploitation of the ores at Lavrion were made of iron processed locally (Conofagos & Papadimitriou, 1981). It is also possible that large amounts of iron were

Received 7 January 2008. Accepted for publication 13 March 2008.
Corresponding author: N. SKARPELIS, Department of Economic Geology and Geochemistry, Faculty of Geology and Geoenvironment, University of Athens, Panepistimiopoli, 157 84 Zografou, Greece. Email: skarpelis@geol.uoa.gr

used for construction purposes in Athenian temples and public buildings (G. Papadimitriou, pers. comm., 2007). Because primary iron ore in the area is lacking, it is concluded that ancient miners exploited gossan. Iron ore was exploited during the post-1864 operations of the Lavrion mines. Approximately 1.5 Mt of iron ore was produced up to 1950 (Argyropoulos, 1955; cited in Marinos & Petrascheck, 1956). The iron ore was exported to Europe for metallurgical processing, because proposed investment in a ferrous metallurgical plant never materialized.

Of special significance for the industrial development of the country in the second half of the 19th century was the processing (calcination) of calamine. The term "calamine" is here used to indicate zinc-rich ore, rather than the discredited mineral name synonymous with smithsonite. Processing of calamine ore took place between 1876 and 1930. The calamine-rich waste from the ancient mining operations along with the exploited raw material was used to produce high-grade zinc oxide in various types of kilns. Exploitation of calamine took place in several mines at Lavrion, with Kamariza being the most important. The calcined calamine was exported to Central Europe for the production of metallic zinc. It is reported that approximately 1.1 Mt of calcined calamine containing 30–60% Zn was produced from 1876 to 1917 (Dermatis, 2000, 2003). Mining activity in Lavrion for base metals and silver was continuous from 1864 to 1978, when the mine was closed due to exhaustion of economic sulfide ore. Recent assessment of the supergene mineral resource at Lavrion is lacking. Although non-sulfide zinc ores are now considered as attractive targets for the mineral industry, extensive historical mining, recent urban development, and the need for protection of significant archaeological, archaeomining and metallurgical sites combine to make Lavrion an unsuitable area for mineral exploration.

This paper describes the geology, mineralogy, and geochemistry of the supergene ores and discusses the origin of supergene ore bodies formed as fillings of vertical to subvertical fractures and of caverns in the marble.

2. Geological background

The Lavrion area is part of the Attic–Cycladic crystalline belt, which is a polymetamorphic terrane within the Alpine orogen of the Hellenides (Fig. 1). The polymetamorphic development of the belt in Oligocene–Miocene times consists of Late Cretaceous (?)–Eocene high pressure/low temperature metamorphism with a greenschist to amphibolite facies overprint (Altherr *et al.*, 1982). Recent studies on metamorphic core complexes exposed in the Cyclades suggest that this regional-scale retrograde overprint of the Cycladic Blueschist Unit was a result of back-arc extension. Large-scale extension in the Aegean was achieved by low-angle normal faulting (e.g. Lister *et al.*, 1984; Avigad *et al.*, 1997). Magma generation, emplacement of plutonic rocks, and minor volcanic activity took place in the Late Miocene. Mineralization in the Cyclades is associated with successive stages of tectono-plutonic evolution and is closely related to the extensional faulting (Skarpelis, 2002). Invasion of marble by ascending hydrothermal fluid and deposition of carbonate-hosted massive sulfide ore (CRDS) accompanied skarn formation associated with contact metamorphism around granitoid intrusions. Late NW–SE-trending tension gashes acted as conduits for ascending hydrothemal fluid with concomitant formation of veins containing barite and base and precious metal sulfides (Fig. 1).

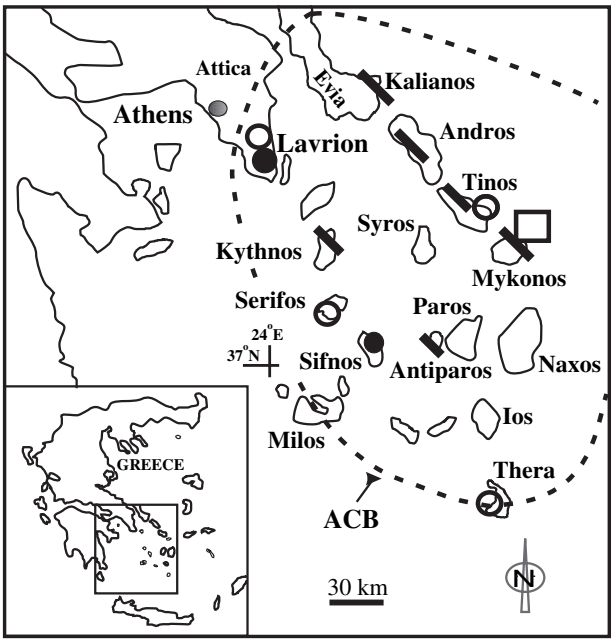

Fig. 1 Miocene ore deposit types in the Attic–Cycladic belt (ACB) (Skarpelis, 2002). (●) Carbonate replacement massive sulfides, (○) skarn, (□) detachment fault-related mineralization, and (—) epithermal veins.

The geology of southeast Attica is dominated by metamorphic and igneous rocks (Fig. 2). The metamorphic rocks belong in two distinct tectonostratigraphic units separated by a detachment fault: a Basal Unit

Fig. 2 Geological map of the Plaka–Kamariza area, Lavrion (from Skarpelis, 2007).

consisting of Lower Marble, a metaclastic subunit (Kaesariani schists), and the Upper Marble; and the overlying Cycladic Blueschist Unit. The detachment fault was active during late Miocene times as deduced from the age of granitoid sills emplaced along and close to the fault plane. U-pb ion microprobe (CSHRIMP) dating of zircons from lensoid orthogneiss bodies in the metaclastic subunit indicates an Early Triassic age for part of the Basal Unit (Liati *et al.*, 2007). Non-metamorphic rocks in the area consist of Late Cretaceous carbonates (Leleu & Neumann, 1969) and Neogene lacustrine and brackish-water deposits (Marinos & Petrascheck, 1956), both tectonically overlying the Blueschist Unit. The igneous rocks of Lavrion are the northwesternmost outcrops of granitoid intrusions in the Attic–Cycladic belt and were emplaced during the Miocene extensional event (Skarpelis *et al.*, 2008). Two distinct rock types are identified: a granodiorite stock cropping out in the Plaka area; and subvertical dikes of porphyritic rocks occurring throughout the Basal Unit (Fig. 2). Intrusion of the granodiorite was accompanied by contact metamorphism of the surrounding "Kaesariani schists" (Baltatzis, 1981). A K-Ar minimum age of 9.4 ± 0.3 Ma was returned by K-feldspar from a dike in the Basal Unit (Skarpelis *et al.*, 2008).

Massive skarn-type base metal sulfide ore containing pyrrhotite is hosted by marble in the contact metamorphic aureole. The ore was exploited for its Ag, Zn, and Pb contents. Low-tonnage, WNW–ESE-trending, Ag-rich, vein-type mineralization is hosted by hydrothermally altered hornfels, and contains a variety of base metal sulfides and Ag-rich sulfosalts (Skarpelis, 2007). The widespread carbonate-hosted massive Pb-Ag-Zn sulfide ore bodies at Lavrion are structurally and lithologically controlled. They are spatially related to the late Miocene detachment fault, shear bands within calcitic marbles, and shear contacts between the marbles and the intercalated metaclastic subunit (Fig. 3). The principal sulfides are pyrite, sphalerite, and galena, accompanied by lesser amounts of chalcopyrite, arsenopyrite and tetrahedrite. Cu-pyrite ore bodies consist mainly of pyrite, arsenopyrite, chalcopyrite plus minor sphalerite, galena and sulfosalts. Fluorite, barite, quartz and carbonate are the gangue minerals. A polymetallic geochemical signature characterizes the mineralization. Lead, Ag, Zn and Cu contents are similar to those of the carbonate-hosted replacement deposits. Galena and tetrahedrite-tennantite are the main Ag carriers. Refractory Au is associated mainly with pyrite and arsenopyrite. Gold content of pyrite–arsenopyrite concentrates and Cu-pyritic ore from mantos ranges from 0.6 to 6 and 1.2 to 5.9 g/t, respectively (Skarpelis, 2007). Fluid inclusion studies show sulfide deposition in the manto-type ore bodies at temperatures of approximately 280°C from fluid

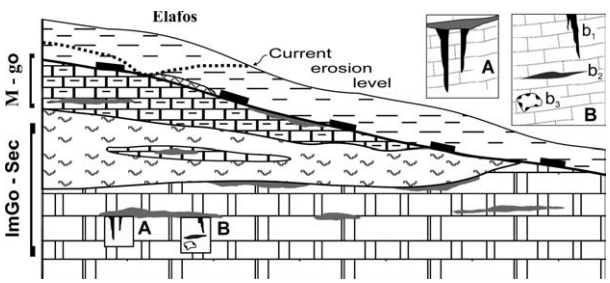

Fig. 3 Schematic geological section (not to scale) (Skarpelis, 2007) showing the setting of the hypogene ore and supergene non-sulfide iron and zinc mineralization in the Kamariza area. (**- - -**) Current erosion level. Most of the mature gossans (M-Go) are located along the detachment fault, whereas both immature gossans and supergene non-sulfide ore bodies (ImmGo-Supg) occur at depth. A, supergene non-sulfide iron ore; B, supergene non-sulfide zinc ore; b_1, open-space filling of joint planes and tension gashes; b_2, stratabound marble replacement; b_3, lining walls of karstic cavities.

with salinities between 14 and 17 wt% NaCl eq. In contrast, fluorite deposition occurred at lower temperatures (125–250°C) from fluid with highly variable salinities (1–19 wt. % NaCl eq.) (Skarpelis *et al.*, 2007).

3. Materials and methods

Sampling of the oxidized ore was conducted in several old underground mining sites at Kamariza, near the Ilarion, Serpieri and J. Baptiste shafts, and at Plaka (Fig. 4). Additional samples of weathered ore from open pit mines at Plaka, Elafos and the "third kilometer" were studied mineralogically. Chip-channel sampling of supergene ore bodies was also carried out. Bulk samples of supergene ore and mineral separates of smithsonite were analyzed commercially at OMAC Labs (Galway, Ireland) using aqua regia digestion and inductively coupled plasma–optical emission spectrometry (ICP-OES). Tin was analyzed on iodide fusion/ICP and Au on fire assay. Purity of smithsonite concentrates was checked on X-ray diffraction. The mineralogy of the supergene ore was studied by the application of conventional X-ray diffraction techniques on bulk samples and on mineral concentrates devoid of goethite and hematite, combined with scanning electron microscopy. A Siemens D-5005 diffractometer with Cu*K*α radiation and a JEOL JSM-5600 scanning electron microscope (SEM) in energy-dispersive mode were used.

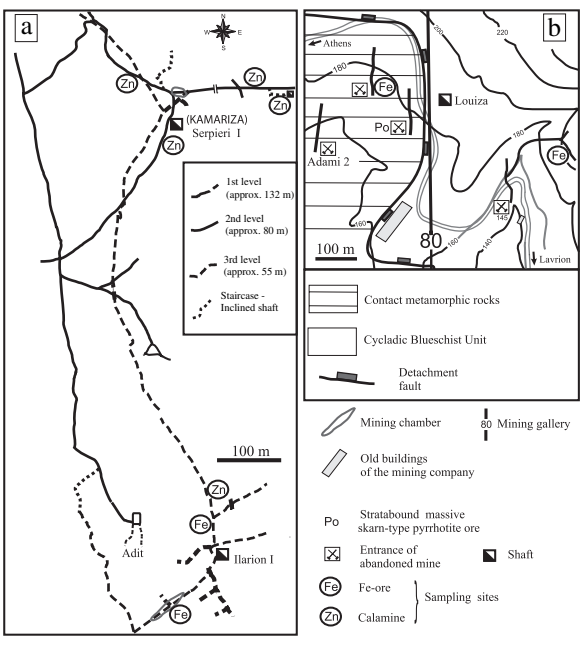

Fig. 4 Maps showing sampling sites of gossan and supergene non-sulfide ore. (a) Kamariza abandoned underground mine; (b) Plaka abandoned mines.

4. Supergene ore

The massive sulfide ore at Lavrion is intensely oxidized as a result of uplift of the Attic–Cycladic belt, progressive erosion of the landscape, development of fractures (tension gashes) under extensional conditions, and consequent weathering of the protore. The current oxidation front at the Kamariza and Plaka mines is at approximately sealevel, because the water table lies at an elevation of approximately +5 m. Mines in the Plaka area, even at the +135-m level, are usually flooded in winter, but the water table drops during the summer and autumn. The oxidized zone observable today may exceed 270 m in thickness, bearing in mind that mining records state that oxidized ore bodies were explored even below sealevel. This thickness estimate is reasonable if it is recalled that at approximately 18,000 BC the sealevel was 125 m lower than at present and that it rose due to global-scale climatic change (Chapell & Charleston, 1986).

Weathering of sulfides continues today and efflorescent salts (e.g. halotrichite, copiapite, hexahydrite, chalcanthite, ferricopiapite, melanterite, rosenite, fibroferrite) are formed at the expense of pyrrhotite and pyrite. Acid mine drainage is evident. Water samples collected from the underground mines of Kamariza and Plaka have pH between 2 and 7. Stagnant or slowly draining waters close to sulfide ore bodies give a pH of approximately 2 and are characterized by strong metal enrichment (Skarpelis *et al.*, 2004). Neoformation of Cu and Zn sulfate minerals (e.g. devilline, ktenasite) and gypsum on the walls of galleries and mining chambers supports mobilization of Zn, Cu and SO_4^{2-} as well. Local mobilization of Fe due to the low pH of descending water is evidenced by the recent formation of goethitic stalactites and limonitic aggregates along vertical to subvertical joints and fissures in the marble. Chemical analyses of groundwater samples from drillholes above the water table show that they are heavily polluted (Stamatis *et al.*, 2001).

Massive sulfide ore bodies unaffected by oxidation are uncommon. Depending on paleo-hydrologic conditions, immature gossan may occur adjacent to the massive sulfide ore bodies in the underground mines. The local geology of individual ore bodies indicates that differences in the depths of oxidation reflect different local paleo-hydrological settings rather than differential

block movements whereby the oxidation profiles could be differentially displaced. More than 400 euhedral to subhedral, coarse- to medium-grained, open-space-filling supergene minerals were identified (for a complete list of Lavrion minerals see Wendel & Rieck, 1999; Baumgaertl & Burow, 2002).

In addition to the immature gossans, supergene ore bodies were explored along tension gashes and joints, and in karstic cavities in marble.

4.1 Gossan

Underground mining at Kamariza was organized through a network of horizontal and inclined galleries and shafts on four main levels: +137, +80, +50 and +30 m, whereas at Plaka there are various levels from +45 to +170 m. Mining involved the "room and pillar" method. Gossan is found on all mine levels, especially at Kamariza. Typical iron-rich gossan is found at and close to the surface as a product of the oxidation of massive sulfide ore on the detachment fault (e.g. Elafos, Thorikos, third kilometer, Sounion). The gossan was collectively described by Marinos and Petrascheck (1956) as "ferromanganese formation".

Several textural gossan types may be identified: colloform, massive, honeycomb and ochre-like (limonite). The gossan is mineralogically and chemically complex, depending on the hypogene mineralogy, the degree of oxidation and leaching of elements and the local hydrologic conditions. Barite, fluorite and quartz remain as relict minerals. The most notable relict mineral is barite, which is relatively unaffected by the acidic environment attending sulfide oxidation (Thornber, 1985) and is residually enriched in the gossan (e.g. Plaka).

The supergene minerals in gossan and partly weathered massive sulfide ore may be broadly classified into the following groups: oxides, hydroxides, sulfates, carbonates and hydroxycarbonates, arsenates, phosphates, silicates and native metals (Table 1). The most abundant are: goethite, hematite, cerussite, anglesite, jarosite, smithsonite, hemimorphite, hydrozincite, plumbojarosite, adamite, azurite, malachite, annabergite, gypsum, scorodite, covellite, beudantite, olivenite, hetaerolite, hydrohetaerolite, Mg-calcite, aragonite, ankerite, ktenasite, cyanotrichite, chalcanthite, brochanthite, chrysocolla, cuprite, and beudantite. Gypsum massively replaces the marble, especially at their lower contact with the ore bodies where it forms massive crystal aggregates locally exceeding 1 m in length. The gypsum formed by attack of the marble

Table 1 Minerals identified in analyzed samples of gossan†

Oxides	
Hematite	Fe_2O_3
Cuprite	Cu_2O
Bismite	Bi_2O_3
Pyrolusite	MnO_2
Hydroxides	
Goethite	α-FeOOH
Psilomelane	$Ba(Mn^{2+}Mn^{4+})_8O_{16}(OH)_4$
Sulfates	
Gypsum	$CaSO_4{\cdot}2H_2O$
Anglesite	$PbSO_4$
Epsomite	$MgSO_4{\cdot}7H_2O$
Hexahydrite	$MgSO_4\cdot6H_2O$
Cyanotrichite	$Cu_4Al_2SO_4(OH)_{12}{\cdot}2H_2O$
Chalcanthite	$CuSO_4{\cdot}5H_2O$
Brochanthite	$Cu_4SO_4(OH)_6$
Copiapite	$Fe^{2+}Fe^{3+}{}_4(SO_4)_6(OH)_2{\cdot}20H_2O$
Jarosite	$KFe^{3+}(SO_4)_2(OH)_6$
Plumbojarosite	$PbFe^{3+}{}_6(SO_4)_4(OH)_{12}$
Beudantite	$PbFe_3AsO_4SO_4(OH)_6$
Serpierite	$Ca(Cu,Zn)_4(SO_4)_2(OH)_6{\cdot}3H_2O$
Tamarugite	$NaAl(SO_4)_2{\cdot}6H_2O$
Melanterite	$FeSO_4{\cdot}7H_2O$
Devilline	$CaCu_4(SO_4)_2(OH)_6{\cdot}3H_2O$
Ktenasite	$(Cu,Zn)_5(SO_4)_2(OH)_6{\cdot}6H_2O$
Rostite‡	$AlSO_4(OH, F){\cdot}5H_2O$
Moorhouseite‡	$(Co,Ni,Mn)SO_4{\cdot}6H_2O$
Peretaite‡	$CaSb_4O_4(OH)_2(SO_4)_2\ 2H_2O$
Khademite‡	$AlSO_4F\cdot5H_2O$
Bieberite‡	$CoSO_4{\cdot}7H_2O$
Carbonates and hydroxycarbonates	
Cerussite	$PbCO_3$
Smithsonite	$ZnCO_3$
Aragonite	$CaCO_3$
Ankerite	$Ca(Mg,Fe^{2+},Mn)(CO_3)_2$
Azurite	$Cu_3(CO_3)_2(OH)_2$
Malachite	$Cu_2(CO_3)(OH)_2$
Rosasite	$(Cu,Zn)_2(CO_3)(OH)_2$
Hydrozincite	$Zn_5(CO_3)_2(OH)_6$
Bismutite	$(BiO)_2CO_3$
Arsenates	
Adamite	$Zn_2AsO_4(OH)$
Olivenite	Cu_2AsO_4OH
Mimetite	$Pb_5(AsO_4)_3Cl$
Scorodite	$Fe^{3+}AsO_4{\cdot}2H_2O$
Manganarsite‡	$Mn^{2+}{}_3AsO_4(OH)_4$
Phosphates	
Monetite‡	$CaHPO_4$
Chalcosiderite‡	$CuFe^{3+}{}_6(PO_4)_4(OH)_8{\cdot}4H_2O$
Chloride	
Sophiite‡	$Zn_2(SeO_3)Cl_2$
Silicates	
Chrysocolla	$(Cu, Al)_2H_2Si_2O_5(OH)_4{\cdot}nH_2O$
Hemimorphite	$Zn_4Si_2O_7(OH)_2{\cdot}H_2O$
Native metals	
Silver	Ag
Bismuth	Bi
Gold	Au

†Formulas from Williams (1990).
‡Identified in Lavrion for the first time.

by acidic SO_4^{2-}-rich meteoric water during protore weathering.

The principal supergene alteration minerals of the sulfides consist of the following: Pyrite and pyrrhotite are replaced by jarosite and goethite. Cerussite, anglesite and plumbojarosite are the main weathering products of galena. Sphalerite was converted to smithsonite, hemimorphite and hydrozincite, along with hetaerolite and goethite. Chalcopyrite and enargite are replaced mainly by chalcocite, goethite, covellite, copper hydroxycarbonates, cuprite, native copper and copper arsenates. Arsenopyrite oxidation resulted in mainly precipitation of scorodite, goethite, mimetite and unidentified hydrous iron arsenates. Gersdorffite is replaced mainly by annabergite. Uncommon supergene native bismuth and gold grains (Ag content approx. 13 wt. %) are dispersed within bismutite–bismite aggregates (Skarpelis, 2002; Solomos *et al.*, 2004).

4.2 Supergene non-sulfide iron and zinc ore

4.2.1 Supergene iron ore

Supergene non-sulfide iron ore normally occurs below sulfide ore bodies or their gossan where they cross-cut stratification and resemble vertical to subvertical (>80°) quadrilateral pyramids (Figs 3, 5a). The iron ore developed in dissolution cavities within the marble, mainly along joint planes and fractures (tension gashes). Structural control of several supergene ore bodies by fractures trending NE–SW was reported by Putzer (1948) and Marinos and Petrascheck (1956). Manto-type sulfide mineralization is cross-cut locally by the supergene mineralization. Iron hydro-/oxides are banded parallel to the walls of the ore bodies, indicating continued dissolution of marble, development of open space and infilling by supergene minerals. Local solution-collapse features are observed. The lengths of the supergene ore bodies exceed tens of meters, whereas their heights range between a few meters and a few tens of meters. Pipe-like Fe-ore bodies, with concentric or rhythmic banding, occur as apophyses of the main supergene bodies. These supergene ore bodies were described as sedimentary mineralization within karst structures by Leleu (1966). The mineralogy of the ores is shown in Table 2. Goethite and hematite are the predominant minerals, whereas smithsonite, adamite, azurite and malachite are the main accessories. Smithsonite fills voids in the iron ore. No relict gangue minerals (e.g. barite, fluorite, quartz) were detected.

Table 2 Minerals identified in the supergene non-sulfide ore bodies

Oxides	
Hematite	Fe_2O_3
Hetaerolite	$ZnMn_2O_4$
Coronadite	$PbMn_8O_{16}$
Hydroxides	
Goethite	α- FeOOH
Nordstrandite	$Al(OH)_3$
Hydrohetaerolite	$Zn_2Mn_4O_8{\cdot}H_2O$
Sulfates	
Gypsum	$CaSO_4 \cdot 2H_2O$
Anglesite	$PbSO_4$
Epsomite	$MgSO_4 \cdot 7H_2O$
Tamarungite	$NaAl(SO_4)_2 \cdot 6H_2O$
Antlerite	$Cu_3SO_4(OH)_4$
Cyanochroite	$K_2Cu(SO_4)_2{\cdot}6H_2O$
Aplowite	$(Co,Mn,Ni)SO_4{\cdot}4H_2O$
Ktenasite	$(Cu,Zn)_5(SO_4)_2(OH)_6{\cdot}6H_2O$
Moorhouseite†	$(Co,Ni,Mn)SO_4{\cdot}6H_2O$
Peretaite†	$CaSb_4O_4(OH)_2(SO_4)_2{\cdot}2H_2O$
Bieberite†	$CoSO_4{\cdot}7H_2O$
Beudantite	$PbFe^{3+}AsO_4SO_4(OH)_6$
Carbonates and hydroxycarbonates	
Smithsonite	$ZnCO_3$
Azurite	$Cu_3(CO_3)_2(OH)_2$
Malachite	$Cu_2(CO_3)(OH)_2$
Hydrozincite	$Zn_5(OH)_6(CO_3)_2$
Hydrous Arsenates	
Adamite	$Zn_2AsO_4(OH)$
Olivenite	$Cu_2AsO_4(OH)$
Chenevixite	$Cu_2Fe^{3+}{}_2(AsO_4)_2(OH)_4{\cdot}H_2O$
Clinoclase	$Cu_3AsO_4(OH)_3$
Picropharmacolite	$Ca_4Mg(AsO_3OH)_2(AsO_4)_2{\cdot}11H_2O$
Manganarsite†	$Mn^{2+}{}_3As_2O_4(OH)_4$
Phosphates	
Chalcosiderite†	$CuFe^{3+}{}_6(PO_4)_4(OH)_8{\cdot}4H_2O$
Monetite†	$CaHPO_4$
Pseudomalachite	$Cu_5(PO_4)_2(OH)_4$
Silicate	
Hemimorphite	$Zn_4Si_2O_7(OH)_2{\cdot}H_2O$

†Identified in Lavrion for the first time.

4.2.2 Supergene zinc ore

The non-sulfide zinc ore occurs mainly as botryoidal concretions filling open space along vertical to subvertical joint planes in the marble, as well as in the form of stratabound bedding plane replacements in marble (Fig. 3). The zinc ore also occurs as botryoidal or globular aggregates coating the walls of karstic cavities in marble (Figs. $3b_1$–b_3, 5b). The principal minerals in the calamine ore at Lavrion are smithsonite, hydrozincite and hemimorphite, with zincian dolomite, calcite, aragonite and goethite as gangue (Skarpelis, 2005). A red-brown band consisting of calcite and zincian dolomite

normally occurs between the host marble and botryoidal smithsonite concretions (Fig. 5b). Vugs into the red-brown band are filled with smithsonite, whereas microcrystalline goethite is interspersed with the dolomite and calcite grains. Beudantite, adamite, hetaerolite, coronadite and hydrohetaerolite are uncommon minerals intergrown with the smithsonite (Fig. 5c–e). Hemimorphite occurs as aggregates of euhedral crystals or as open-space fillings in the smithsonite encrustations (Fig. 5f). Hydrozincite post-dates deposition of smithsonite and occurs as thin whitish crusts on the botryoidal concretions. Botryoidal concretions of calcite and aragonite are common in karstic cavities. Microprobe analyses of smithsonite show minor substitution of Zn by Ca, Fe, Mn and Cd. Chemical analyses of concentrates, and SEM indicate that the yellow smithsonite variety from Kamariza is characterized by high Cd, Fe and Mn content, whereas the blue variety has high Cd and Cu (Table 3). These data agree with the results of the combined mineralogical–microchemical

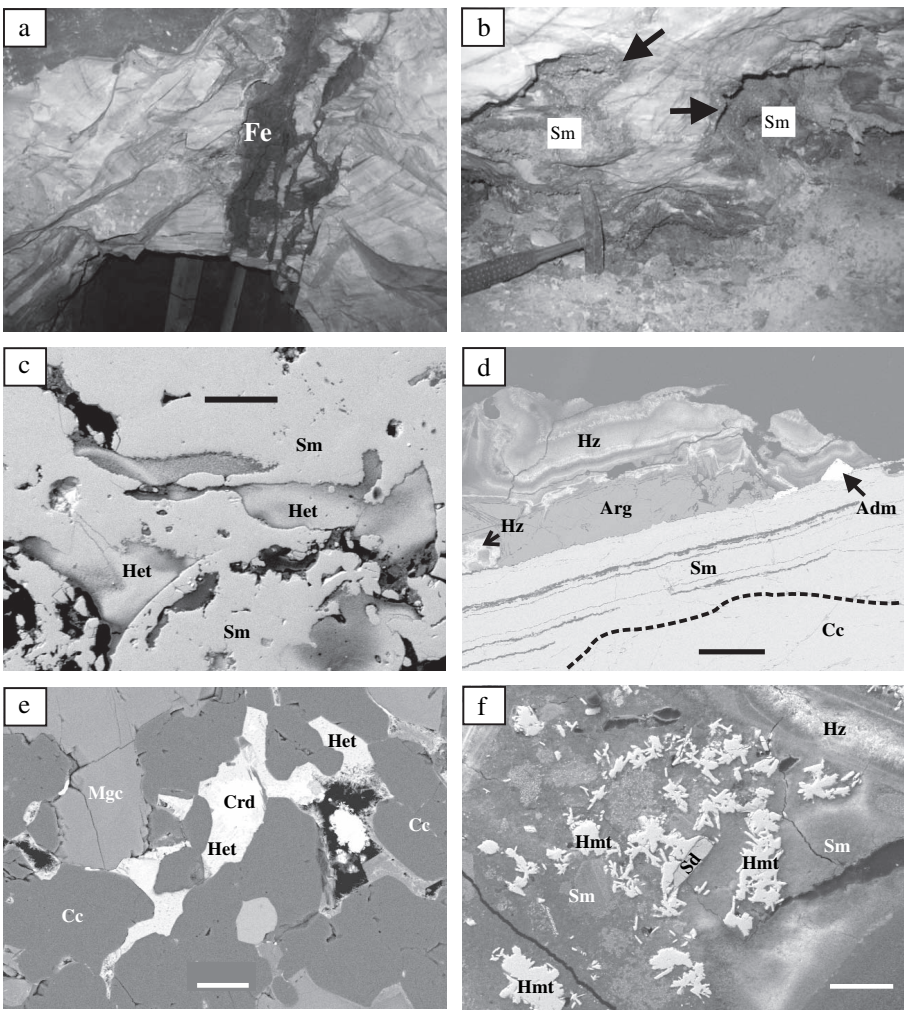

Fig. 5 (a) Supergene iron ore (Fe) along a tension gash in marble (Kamariza mine, Ilarion shaft). (b) Botryoidal smithsonite (Sm) on the wall of karstic cavity. The arrows show a dark grey band made up mainly of calcite, zincian dolomite and disseminated goethite. (c) Hetaerolite (Het) coexisting with smithsonite (Sm) in fissure-filling zinc ore (Kamariza mine). Bar, 100 μm. (d) Aragonite band (Arg) with adamite (Adm) and hydrozincite coating (Hz) on smithsonite encrustations (Sm) replacing calcitic marble (Cc). Bar, 100 μm. (e) Coronadite (Crd) and hetaerolite (Het) filling voids in Mg-calcite (Mgc) and calcite (Cc) in marble. Bar, 20 μm. (f) Aggregates of euhedral hemimorphite crystals (Hmt) in smithsonite encrustations (Sm). Siderite (Sd) is relict. Note the thin hydrozincite crust (Hz). Bar, 50 μm. (c–f) Scanning electron microscope secondary micrographs.

Table 3 Chemical analyses of smithsonite concentrates

Sample no	Fe %	Cu μg g^{-1}	Cd μg g^{-1}	Mn μg g^{-1}
3 (yellow)	0.13	78	3261	1424
7 (blue)	0.03	1489	2629	428

investigation on smithsonite color (Frisch *et al.*, 2002): Cd and Fe in solid solution are the coloring agents in yellow smithsonite, whereas Cu accounts for the blue variety, and Cu and Mn for the greenish variety.

5. Geochemistry

The grade of the supergene mineralization is highly variable, ranging from iron ore to low-grade calamine. The descriptive chemical statistics for bulk samples of gossan and supergene non-sulfide ore are presented in Table 4. Most samples of iron ore have a median Fe content of 50.5 wt%. Samples rich in calamine yielded Zn values up to 38 wt% and moderate Cd contents. Average sulfur contents are low: 0.2 wt% and 0.1 wt% in gossan and supergene ore samples, respectively. Both ore types are enriched in Cu, whereas the As content is low. Silver, Bi, Co, Ni, Sb, Mn, P, Au, Sn, Mo, Mn and Tl concentrations are extremely low.

Varying element mobility, under changing Eh and pH conditions as oxidizing water percolates downwards and alteration of the primary minerals progresses, explains the enrichment or depletion of the supergene ore. In Figure 6, a plot of normalized concentrations of 13 elements, the enrichment/depletion factor, τ, is calculated as:

$$\tau_{(SO/GO)} = C_{SO} / C_{GO} - 1$$

where *C* represents the mean concentration of an element in the supergene ore (SO) or gossan (GO) samples. The most enriched elements in the supergene non-sulfide ore are As, Cu, Cd and Zn, whereas Pb, Mg, Mn and S partly remain in the gossan, indicating incomplete leaching.

Table 4 Descriptive chemical statistics for bulk samples of gossan and supergene non-sulfide ore

Element	Mean	Median	SD	Minimum	Maximum
Gossan samples (n = 12)					
Fe (%)	44	51	16	14	58
Zn (%)	6.0	3	11	0.02	38
Cu (%)	0.4	0.1	0.5	0.01	1.3
Pb (%)	0.8	0.2	1.5	0.01	4.9
Ca (%)	0.7	0.4	1.1	0.2	4.3
Mg (%)	1.4	0.1	4.7	0.04	16
Mn (%)	1.0	0.1	1.6	0.01	3.9
As (%)	0.8	0.5	0.9	0.01	3.0
S (%)	0.2	0.1	0.2	0.05	0.6
P (%)	0.1	0.1	0.04	0.02	0.2
Cd (μg g^{-1})	226	94	318	5	933
Co (μg g^{-1})	105	33	217	13	780
Ni (μg g^{-1})	58	60	39	8	112
Sb (μg g^{-1})	156	29	281	20	978
Supergene ore samples (n = 9)					
Fe (%)	43	49	13	23	56
Zn (%)	11	5	13	2	35
Cu (%)	1	1	1	0.3	3
Pb (%)	0.05	0.01	0.06	0.01	0.19
Ca (%)	0.5	0.5	0.2	0.3	0.7
Mg (%)	0.2	0.1	0.1	0.1	0.4
Mn (%)	0.2	0.2	0.2	0.04	0.8
As (%)	2	2	1	0.4	3
S (%)	0.07	0.06	0.02	0.05	0.1
P (%)	0.08	0.08	0.02	0.04	0.1
Cd (μg g^{-1})	496	148	686	28	1686
Co (μg g^{-1})	39	41	15	18	61
Ni (μg g^{-1})	58	55	32	21	111
Sb (μg g^{-1})	98	51	103	20	315

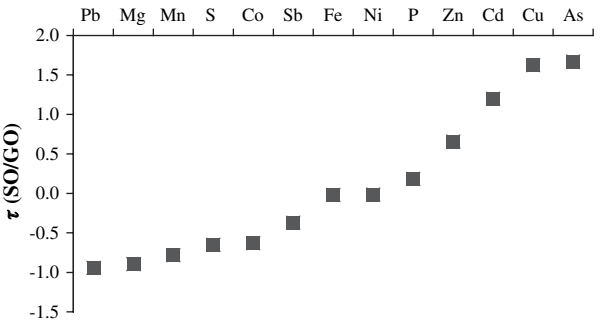

Fig. 6 Plot of normalized concentrations (τ (SO/GO)) of 13 elements, showing enrichment or depletion in the supergene ore.

Element associations in rock samples were further explored by calculating Pearson correlation coefficients for the gossan and supergene ore samples. Multivariate cluster analysis was subsequently applied to the data in order to examine the classification of element groups and recognize any relationships among them. The distance measure used in cluster analysis was the Pearson correlation coefficient at the 95% confidence level. The results of the analysis are shown as dendrograms (Fig. 7). The similarity axis represents the degree of association between the variables, the greater the value the more significant the association.

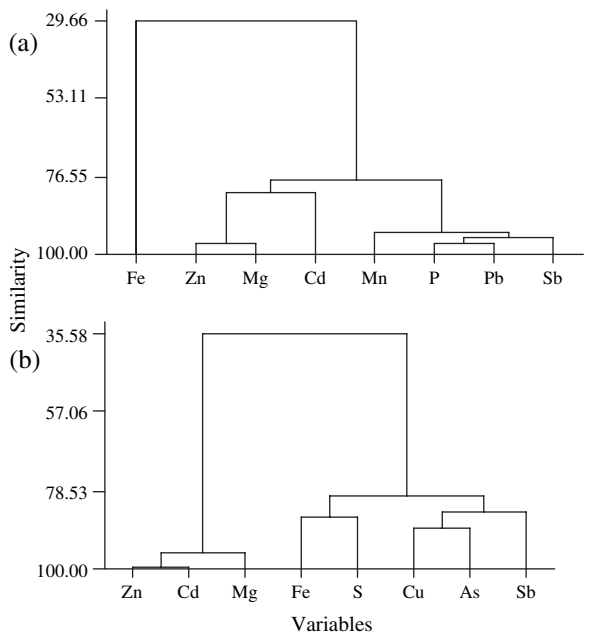

Fig. 7 Dendrograms constructed by hierarchical cluster analysis of variables in (a) gossan and (b) supergene non-sulfide ore samples.

Three distinct clusters can be identified in the gossan samples: cluster I containing Zn, Mg and Cd; cluster II containing Mn, P, Pb and Sb; and cluster III containing Fe. The similarity between clusters I and II has a value of 76.6, indicating a strong association between all the involved elements. The clustering of Fe has a much lower similarity value of 29.6, probably reflecting the predominance of Fe oxides in the samples. The dendrogram for the supergene ore samples has two distinct clusters: cluster I containing Zn, Cd and Mg, with a stronger association between Zn and Cd (similarity almost 100%), reflecting the chemical composition of smithsonite; and cluster II containing Fe, S, Cu, As and Sb. This cluster is further subdivided into two: an Fe, S group, probably controlled by Fe-rich sulfosalts in the samples; and a Cu, As, Sb group reflecting the strong association of these elements in the supergene minerals. The relatively low similarity value of 35.5 between clusters I and II may be attributed to different metal solubilities causing Zn to separate from the rest of the elements due to its dissolution, transport and re-precipitation. Such multicyclic oxidation and leaching with enhancement of metal separation was described by Hitzman *et al.* (2003) as being typical in manto-type, carbonate-replacement sulfide deposits, the result being wall-rock replacement by non-sulfide Zn deposits.

6. Discussion

6.1 Origin

The geological setting and mineralogical, textural and geochemical features of the supergene Fe-rich and Zn-rich ores provide strong evidence favoring an origin by oxidation of hypogene sulfide minerals, marble replacement by acidic solutions, and transport of mobile elements and their re-precipitation in secondary trap sites. The absence of the common gangue minerals, such as quartz, barite and fluorite, in the supergene ores provides further evidence. The calamine ores may be classified as Type I in the scheme for non-sulfide zinc deposits proposed by Large (2001).

There is little evidence with which to constrain the age of the supergene mineralization. The district geology suggests that the various ore types at Lavrion were formed in the late Miocene. Rapid surface uplift as a result of extensional tectonics, high denudation rates and relief formation in Attica during the Turolian and Pliocene is evidenced by the occurrence of detrital rock and mineral components originated from both the Cycladic Blueschist and the Basal Unit in terrestrial and lacustrine sediments formed during that time (Mposkos

et al., 2007). Descent of the water table below the detachment fault promoted supergene processes. Hence, supergene ores at Lavrion may have started to form as early as the Pliocene. In this regard most of the sulfide ore bodies associated with the late Miocene extensional faulting and hydrothermal activity in the Cycladic islands are characterized by thick oxidized zones (e.g. Kythnos, Mykonos, Sifnos) (Skarpelis, 2002); hence they were an attractive iron and oxide copper resource in ancient times (e.g. the Kythnian oxide copper ore mined since the early Bronze age).

Formation of gossan resulted in the release of major and trace elements from the original sulfides, and their mobilization to varying degrees. Oxidation and breakdown of sulfide minerals under the influence of oxygenated groundwater caused significant change in the pH–Eh environment both within and beneath the ore bodies. When the pH of the infiltrating ground and surface water declines, as a result of sulfide and Fe^{2+} oxidation, the concentration of metals released into the drainage water usually increases. The porphyritic dike rocks and metapelite layers were also attacked by acidic waters, resulting in Al mobilization and formation of assemblages containing halloysite, nordstrandite, gibbsite and kaolinite.

The acidic water reacted with the carbonate host rocks, leading to pH reduction. Deposition of the supergene ore was controlled by major zones of marble dissolution, mainly along fractures and joints. Tension gashes and joints in the host marble also facilitated percolation of oxygenated waters to a depth enabling oxidation of the hypogene ore. Infiltration of acidic water beneath the active sulfide oxidation zone and its downward percolation within the marbles resulted in progressive leaching of the carbonates, development of cavities and contemporaneous reduction in the concentration of dissolved metals because, under near-neutral pH conditions, most of the metals are either adsorbed onto mineral surfaces or precipitate as discrete mineral species. The intensity and extent of the oxidation are plausibly explained by the high proportion of pyrite in the massive sulfide ore and the high As and Fe content of the pyrite and sphalerite, respectively (Skarpelis, 2007). The relatively high iron and zinc content of the supergene ore bodies probably indicates that most precursor sulfide ores were highly pyritic. Acid production during pyrite oxidation causes intense leaching of the oxidizing ore and promotes mobilization of metals into the groundwater (e.g. Châvez, 2000; Sillitoe, 2005). In sulfide ores where pyrite is only a minor component, acid leaching is not as severe and higher concentrations of trace metals remain in the resulting gossan (Andrew, 1984). The high acid-generating capacity of oxidizing pyrite would assist in leaching zinc from the protore. Indeed, the presence of sufficient Fe-sulfide in the hypogene mineralization is considered by Large (2001) as a critical factor for efficient sulfide oxidation and preservation of the supergene zinc minerals.

On the basis of data of the mineralogy and chemical composition of the hypogene sulfide ores (Skarpelis, 2007), element redistribution in the supergene environment is evident. But although the sulfide ore is Pb rich, the supergene ore has a very low Pb content. During the oxidation process, Pb is retained as anglesite or cerussite, depending on the relative activities of sulfate ions and carbonate species in the meteoric water (Sangameshwar & Barnes, 1983), but it also enters the structure of many supergene phases (e.g. plumbojarosite, pyromorphite, beudantite). The low Pb content in supergene non-sulfide ores is a result of the relative immobility of the metal in drainage waters with pH<6, as proposed by Mann and Deutscher (1980). In contrast, the elements that are enriched in the supergene non-sulfide ore are leached from the hypogene sulfide minerals and remain in solution until the pH is sufficiently buffered by the surrounding carbonate rock for supergene minerals to precipitate (e.g. smithsonite). Arsenic is enriched in the zinc-rich non-sulfide ore by a factor of 1.7. This observation, in conjunction with the presence in the gossan of scorodite, a metastable As mineral precipitating under low-pH, oxidizing conditions (Dove & Rimstidt, 1985), indicates that the mobility of As is probably controlled by the increasing solubility of scorodite with increasing pH. Zhu and Merkel (2001) estimated that scorodite has the lowest solubility at a pH between 5.0 and 5.8, and that its increased solubility at higher pH is accompanied by reduction in solution Eh. Under these conditions, the concentration of total As is controlled simultaneously by incongruent dissolution of scorodite and absorption of arsenate onto the iron hydroxides that are produced.

The major hypogene source of Cu is chalcopyrite and copper-bearing sulfosalts, whereas the As is released during the oxidation of arsenopyrite, As-rich pyrite, löllingite and As-bearing sulfosalts. Under conditions of low pH, arsenopyrite oxidizes rapidly and forms highly soluble arsenic compounds as well as Fe^{2+} or Fe^{3+} arsenites or arsenates (Richardson & Vaughan, 1989). Oxidation of sphalerite-rich mineralization leads to the release of Fe, Cd, Mn and associated trace elements (e.g. In, Ge, Ga). The major source

of manganese is sphalerite (mean mole% MnS of 0.83 and 0.12 in skarn and manto-type ore, respectively). The primary source of Cd is sphalerite because hypogene greenockite is uncommon. The strong geochemical correlation between Zn and Cd in the calamine ore indicates that the Cd is fixed mainly in the smithsonite. Supergene Cd-bearing minerals (e.g. niedermayrite, otavite) are only minor constituents of the ore. Greenockite, where it occurs as coatings on smithsonite or in close association with oxidized sphalerite, may be of supergene origin because it is stable in acidic solutions under weakly oxidizing or reducing conditions (Takahashi, 1960). Indium is contained in roquesite, sphalerite and Cu-sulfides and sulfosalts. The rare indium hydroxide dzhalindite has been identified. Cobalt, Ni and Au are liberated from the crystal lattice of arsenopyrite and pyrite in the course of weathering, whereas Ag, Sb and Bi are derived mainly from galena and the sulfosalts. The low Au content of the gossan and the supergene non-sulfide mineralization compared with that of the hypogene ore suggests liberation and chemical remobilization of the element during oxidation of gold-bearing sulfides. It further suggests that Au was not re-precipitated in the supergene environment. In the presence of carbonate buffer, as in the case of Lavrion marble, Au mobilization is possible as a thiosulfate complex (Zeegers & Leduc, 1993 and references therein). The source of phosphorus is attributed to destruction of phosphates in the host marble or accessory apatite of the sulfide ore. Metapelite layers in the marble or the "Kaesariani schists" may be a potential vanadium source for the uncommon supergene vanadates (e.g. descloizite).

6.2 Physicochemical conditions of deposition

Using data provided mainly by Vink (1986), Magalhaes *et al.* (1988) and Williams (1990) we attempt an approximate evaluation of depositional conditions for the supergene ore.

The neutralizing species in the ore-hosting rocks are calcite, magnesium-bearing carbonates and minor phosphates (apatite gangue and minor phosphates in the country rocks). Iron oxyhydroxides can precipitate and persist over a wide pH range, with goethite dominating at values of 3–6, but easily transformed to hematite upon dehydration (Thornber & Wildman, 1984). The lack of jarosite in the supergene iron ore bodies indicates that the pH of the drainage waters was >3 (McGregor & Blowes, 2002). Zinc is the most mobile of the base metals, and in solutions containing sulfate, carbonate, hydroxyl and chloride anions $ZnSO4^0$ and $Zn(OH)_2^0$ are the dominant complex ions, while $ZnCO_3$, $Zn(OH)_2$ and $Zn_4(SO_4)(OH)_6$ are the phases limiting Zn solubility (Mann & Deutscher, 1980). The solubility of zinc hydroxide is not related to the total content of carbon dioxide in solution, but is a function of pH. The occurrence of smithsonite in the supergene ore bodies indicates that the acidic, SO_4^{2-}-rich waters became less acidic during water–marble interaction, causing precipitation of Zn species such as $ZnCO_3$. Smithsonite is stable at intermediate to high pH values buffered by the carbonate host rocks and high P_{CO2} conditions. The predominance of smithsonite over hydrozincite suggests relatively high P_{CO2} (Williams, 1990; Boni *et al.*, 2003). Smithsonite is least soluble in natural waters that have a pH between 6 and 8 (Takahashi, 1960). Precipitation of azurite and malachite from cupric ion-bearing solutions takes place at pH between 6 and 8, depending on CO_2 partial pressures, with malachite being the stable carbonate phase under atmospheric conditions and azurite crystallizing at equilibrium under somewhat more elevated pressures of CO_2, under lower pH and within a narrow zone of Cu^{2+} activity (between log $a Cu^{2+}$ –5 and –2) (Symes & Kester, 1984; Vink, 1986). The local occurrence of smithsonite apart from malachite might be a result of Cu activity in solution and the overall greater mobility of Zn^{2+} versus Cu^{2+} ions in the supergene environment (Mann & Deutscher, 1980). The occurrence of secondary phosphates (e.g. pseudomalachite) shows the stability of pentavalent phosphorus (PO_4^{3-}) throughout the supergene environment. Pseudomalachite is stable under neutral to slightly acidic pH conditions (approx. 7–3), depending on the activity of Cu^{2+} (Magalhaes *et al.*, 1986), a conclusion in accord with the occurrence of pseudomalachite in *in situ* oxidized zones of some porphyry copper deposits (e.g. Radomiro Tomic, Chile; Cuadra & Rojas, 2001). Gypsum and minor amounts of complex sulfates (e.g. cyanochroite) were formed during the same process. Arsenic occurs mainly with Cu, Fe and Pb as chenevixite, clinoclase, and beudantite and with Zn as adamite. Clinoclase and olivenite form under a wide range of neutral–slightly acidic pH conditions and Cu^{2+} activities from appropriate supergene solutions. Olivenite crystallizes at higher copper and arsenate concentrations and lower pH relative to clinoclase (Magalhaes *et al.*, 1988). Of the two intermediate members of the paragenetic sequence, clinoclase cornwallite cornubite olivenite, only the second occurs uncommonly at Lavrion. Because the paragenetic relations of the cornwallite to the other members of the

sequence is unknown, an evaluation of pH conditions is impossible. Further research is needed to evaluate the possibility of As adsorption onto goethite and hematite. Adamite is a common mineral in the ore bodies as a result of the wide range of chemical conditions (pH 3–7) under which it is stable (Williams, 1990). The occurrence of hemimorphite in the calamine ore along with the minor silica detected in supergene ore bodies shows that silica was released and mobilized, from silicate minerals in the dike rocks, the Kaesariani schists and impure marble layers. Breakdown of silicate minerals resulting from acid attack during the gossan-forming process results in supersaturation in SiO_2 in drainage waters and precipitation of supergene silicates and silica (Thornber, 1985).

The effect of weathering and supergene processes at Lavrion is also recorded in groundwater quality. The lithological characteristics of Lavrion rocks combined with local tectonic structures and the extensive underground mine workings provide appropriate hydrogeological conditions for groundwater movement. Specifically, carbonate formations, the lower and upper marble, that compose the main aquifer have high permeability due to the intense fracturing that aided karst development. The present water table, lying approximately 5 m above sealevel, has an eastward hydraulic gradient towards the sea. High heavy metal (Pb, Cd, Zn, Ni) concentrations were measured in groundwater samples collected within the historical Lavrion mining area by Stamatis *et al.* (2001). Interestingly, in their factor analysis model, Zn is separated from the rest of the elements, suggesting that a different process controlled Zn solubility.

7. Conclusions

The supergene iron ore and calamine at the Lavrion deposit were formed by supergene processes involving downward-penetrating water, oxidation of hypogene sulfide mineralization, partial mobilization of elements and their re-precipitation in open spaces developed by interaction of acidic water with marble. Part of the iron in the pyritic portion of the sulfide ore remained as gossan. The age of the supergene ore is poorly constrained, but presumably Pliocene. Mineral deposition was controlled mainly by pH conditions, P_{CO2}, metal ion activities (e.g. $a(Cu^{2+})$, $a(Zn^{2+})$ and $a(SO_4^{2-})$ and Eh. Formation of supergene minerals took place under near-neutral to mildly acidic conditions. Further experimental work, however, on paragenetic sequences and equilibrium models, particularly relevant to sulfate and arsenate minerals, is clearly required to better constrain the physicochemical conditions of deposition of the various mineral assemblages.

Weathering processes acting on the Lavrion massive sulfide ore resulted in the formation of supergene ore bodies, including beautiful mineral specimens, several of them with Lavrion as the type locality (e.g. serpierite, niedermayrite, ktenasite, kapelassite). Gossan formation had a strong negative impact on the environment, whereas the formation of the supergene ore bodies was important from an environmental point of view because large quantities of toxic metals and oxyanions were fixed in the supergene minerals, resulting in a significant Fe and Zn resource.

In mode of occurrence and origin, the Lavrion calamine ore is similar to most of the non-sulfide zinc deposits described by Hitzman *et al.* (2003), Boni and Large (2003) and Boni *et al.* (2003).

Acknowledgments

Financial support to the senior author from the Special Account for Research Grants, National and Kapodistrian University of Athens is gratefully acknowledged. We wish to thank Evangelos Michailides and Stavros Triantafyllidis (Department of Economic Geology and Geochemistry) for assistance with the SEM work. Thanks are also due to the B′ Ephorate of Prehistoric and Classic Antiquities in Athens for permitting access to the Kamariza underground mines. Authors sincerely thank Dr Richard Sillitoe and an anonymous reviewer for thorough review and helpful comments. The senior author thanks Stathis Lazaridis and Karl Heinz Fabritz for help during visits to the abandoned underground mines.

References

Altherr, R., Kreuzer, H., Wendt, I., Lenz, H., Wagner, G. A., Keller, J., Harre, W. and Hohndorf, A. (1982) A late Oligocene/early Miocene high temperature belt in the Attic-Cycladic crystalline complex (SE Pelagonian, Greece). Geol. Jahrb., E23, 97–164.

Andrew, R. L. (1984) The geochemistry of selected base-metal-gossans, southern Africa. J. Geochem. Explor. 22, 161–192.

Avigad, D., Garfunkel, Z., Jolivet, L. and Azanon, J. M. (1997) Back arc extension and denudation of Mediterranean eclogites. Tectonics, 16, 924–941.

Baltatzis, E. (1981) Contact metamorphism of a calc-silicate hornfels from Plaka area, Laurium, Greece. Neues Jahrb. Miner. Monats., 11, 481–488.

Baumgaertl, U. and Burow, J. (2002) Laurion: Die Mineralien von A bis Z. Aufschluss, 53, 278–362.

Boni, M. and Large, D. (2003) Nonsulfide zinc mineralization in Europe: An overview. Econ. Geol., 98, 715–729.

Boni, M., Gilg, H. A., Aversa, G. and Balassone, G. (2003) The "Calamine" of southwest Sardinia: Geology, mineralogy, and stable isotope geochemistry of supergene Zn mineralization. Econ. Geol., 98, 731–748.

Chapell, J. and Charleston, N. J. (1986) Oxygen isotopes and sea level. Nature, 324, 137–140.

Châvez, W. X. Jr. (2000) Supergene oxidation of copper deposits: Zoning and distribution of copper oxide minerals. Soc. Econ. Geol. Newsl., 41, 1, 10–21.

Conofagos, K. (1980) The Ancient Laurium and the Greek technique for silver production. Ekdotiki Athinon, Athens, 458p (in Greek).

Conofagos, K. and Papadimitriou, G. (1981) La technique de production de fer et d' acier par les Grecs anciens en Attique pendant la période classique. Proc. Acad. Athens, 56, 148–172.

Cuadra, P. and Rojas, G. (2001) Oxide mineralization at the Radomiro Tomic porphyry copper deposit, northern Chile. Econ. Geol., 96, 387–400.

Dermatis, G. (2000) La production de calamine calcinée (1875–1917) de la Compagnie Francaise des mines du Laurium. Le programme avec la Société Grecque de métallurgie du fer (1899–1902). Mineral Wealth, 117, 51–58 (in Greek with French abstract).

Dermatis, G. (2003) Lavrion: The mining and metallurgical industry during 1860–1917. Edition by the "Technological and Cultural Park of Lavrion", National Technical University of Athens (in Greek), Athens, 562p.

Dove, P. M. and Rimstidt, J. (1985) The solubility and stability of scorodite, $FeAsO_4{\cdot}2H_2O$. Am. Mineral., 70, 838–844.

Frisch, P. L., Lueth, V. W. and Hlava, P. F. (2002) The colors of smithsonite: A microchemical investigation. New Mexico Geology, 24, 132–133.

Hitzman, M. W., Reynolds, N. A., Sangster, D. F., Allen, C. R. and Carman, C. E. (2003) Classification, genesis, and exploration guides for nonsulfide zinc deposits. Econ. Geol., 98, 685–714.

Large, D. (2001) The geology of non-sulphide zinc deposits: An overview. Erzmetall, 54, 264–276.

Leleu, M. (1966) Les gisements plombo-zincifères du Laurium (Grece). Sci. Terre, XI, 3, 293–343.

Leleu, M. and Neumann, M. (1969) L' âge des formations d' Attique: Du Paléozoique au Mésozoique. C.R. Acad. Sci. Paris, 268, 1361–1363.

Liati, A., Skarpelis, N. and Pe-Piper, G. (2007) Deciphering the time of igneous activity in the Lavrion ore province, Attica, Greece: Manifestation of late Miocene and Triassic magmatism. Goldschmidt 07 Annual Conference. Geochim. Cosmochim. Acta, 71(Suppl 15S), p. 578.

Lister, G. S., Banga, G. and Feenstra, A. (1984) Metamorphic complexes of Cordilleran type in the Cyclades, Aegean Sea, Greece. Geology, 12, 221–225.

Magalhaes, M. C. F., Pedrosa de Jesus, J. and Williams, P. A. (1986) Stability constants and formation of Cu(II) and Zn(II) phosphate minerals in the oxidised zone of base metal orebodies. Mineral Mag., 50, 33–39.

Magalhaes, M. C. F., Pedrosa de Jesus, J. and Williams, P. A. (1988) The chemistry of formation of some secondary arsenate minerals of Cu(II), Zn(II) and Pb(II). Mineral Mag., 52, 679–690.

Mann, A. W. and Deutscher, R. L. (1980) Solution geochemistry of lead and zinc in water containing carbonate, sulphate and chloride ions. Chem. Geol., 29, 293–311.

Marinos, G. P. and Petrascheck, W. E. (1956) Laurium. Geol. Geophys. Res., Institute for Geology and Subsurface Research. Geol., Athens, 4, 1, 1–247.

McGregor, R. G. and Blowes, D. W. (2002) The physical, chemical and mineralogical properties of three cemented layers within sulfide-bearing mine tailings. J. Geochem. Explor., 76, 195–207.

Mposkos, E., Krohe, A., Diamantopoulos, A. and Baziotis, I. (2007) Late- and post-Miocene geodynamic evolution of the Mesogea basin (east Attica, Greece): Constraints from sediment petrography and structures. Bull. Geol. Soc. Greece, 40, 399–411.

Putzer, H. (1948) Die Erzlagerstaette von Lavrion. Ann. Geol. Pays Hellen, II, 1, 16–46.

Richardson, S. and Vaughan, D. J. (1989) Arsenopyrite: A spectroscopic investigation of altered surfaces. Mineral Mag., 53, 223–229.

Sangameshwar, S. R. and Barnes, H. L. (1983) Supergene processes in zinc-lead-silver sulfide ores on carbonates. Econ. Geol., 78, 1379–1397.

Sillitoe, R. H. (2005) Supergene oxidized and enriched porphyry copper and related deposits. In Hedenquist, J. W., Thompson, J. F. H., GoldFarb, R. J. and Richards, J. P. (eds.), Economic Geology 100th Anniversary Volume, Society of Economic Geologists, Littleton, 723–768.

Skarpelis, N. (2002) Geodynamics and evolution of the Miocene mineralization in the Cycladic–Pelagonian Belt, Hellenides. Bull. Geol. Soc. Greece, 34, 6, 2191–2206.

Skarpelis, N. (2005) Non-sulfide zinc ores in Lavrion, Greece. In Volume of Abstracts, Exploratory Workshop "Non-Sulfide Zn-pb Ores: Genetic Models and Exploration: The European Deposits, European Science Foundation, Iglesias (Sardinia), p. 34.

Skarpelis, N. (2007) The Lavrion deposit: Geology, mineralogy and minor elements chemistry. Neues Jahrb Miner. Abh., 183/3, 227–249.

Skarpelis, N., Triantafyllidis, S. and Baziotis, J. (2004) Acid rock drainage in the mine of Lavrion, Greece. *In* Agioutantis, Z. and Komnitsas, K. (eds.) International conference "Advances in mineral resources management and environmental geotechnology", Hania, Greece. Milos Conferrences, Athens, 531–536.

Skarpelis, N., Lüders, V. and Banks, D. (2007) Fluid inclusions, REE and sulfur isotope geochemistry of the Lavrion carbonate hosted ore deposit, SE Attica, Greece. Goldschmidt 07 Annual conference. Geochim. Cosmochim. Acta, 71(Suppl 15S), p. 945.

Skarpelis, N., Tsikouras, B. and Pe-Piper, G. (2008) The Miocene igneous rocks in the Basal Unit of Lavrion (SE Attica, Greece): Petrology and geodynamic implications. Geol. Mag., 145, 1, 1–15.

Solomos, Ch., Voudouris, P. and Katerinopoulos, A. (2004) Mineralogical study of bismuth–gold–antimony mineralization at the area of Kamariza, Lavrion. Bull. Geol. Soc. Greece, 36, 387–396 (in Greek with English abstract).

Stamatis, G., Voudouris, K. and Karefilakis, F. (2001) Groundwater pollution by heavy metals in historical mining area of Lavrion, Attica, Greece. Water, Air Soil Pollut., 128, 61–83.

Symes, J. L. and Kester, D. R. (1984) Thermodynamic stability studies of the basic copper carbonate mineral, malachite. Geochim. Cosmochim. Acta, 48, 2219–2229.

Takahashi, T. (1960) Supergene alteration of zinc and lead deposits in limestone. Econ. Geol., 55, 6, 1083–1115.

Thornber, M. R. (1985) Supergene alteration of sulphides VII. Distribution of elements during the gossan-forming process. Chem. Geol., 53, 279–301.

Thornber, M. R. and Wildman, J. E. (1984) Supergene alteration of sulphides, VI. The binding of Cu, Ni, Zn, Co and Pb with iron-bearing gossan minerals. Chem. Geol., 44, 399–434.

Vink, B. W. (1986) Stability relations of malachite and azurite. Mineral Mag., 50, 41–47.

Wendel, W. and Rieck, B. (1999) Lavrion: Die komplette mineralliste. Lapis, 24, 7–8, 61–67.

Williams, P. A. (1990) Oxide zone geochemistry. Ellis Horwood, Chichester, 286p.

Zeegers, H. and Leduc, C. (1993) Geochemical exploration for gold in temperate, arid, semi-arid, and rain-forest terrains. *In* Foster, R. P. (ed.) Gold metallogeny and exploration. Chapman and Hall, London, 309–335.

Zhu, Y. and Merkel, B. J. (2001) The dissolution and solubility of scorodite, $FeAsO_4 \cdot 2H_2O$: Evaluation and simulation with PHREEQC2. Wiss. Mitt. Inst. für Geologie, Technische Universitaet Bergakademie Freiberg, 18, 72–87.